Modular Multi-Rotors: From Quadrotors to Fully-Actuated Aerial Vehicles

Supplementary Materials

Jiawei Xu[1*], Diego S. D'Antonio[1] and David Saldaña[1]

[1*]Computer Science and Engineering, Autonomous and Intelligent Robotics Laboratory (AIRLab), Lehigh University, 113 Research Drive, Bethlehem, 18015, PA, USA.

*Corresponding author(s). E-mail(s): jix519@lehigh.edu;
Contributing authors: diego.s.dantonio@lehigh.edu; saldana@lehigh.edu;

1 Proof: $\boldsymbol{T}$-Modules are torque-balanced

$$\textstyle\sum_{j=1}^{4} \boldsymbol{p}_j \times {}^{M}\boldsymbol{R}_j \hat{\boldsymbol{z}} = \boldsymbol{0}, \tag{1}$$

$$\textstyle\sum_{j=1}^{4} {}^{M}\boldsymbol{R}_j (-1)^j \hat{\boldsymbol{z}} = \boldsymbol{0}, \tag{2}$$

$$\textstyle\sum_{j=1}^{4} {}^{M}\boldsymbol{R}_j \hat{\boldsymbol{z}} = \lambda \boldsymbol{R}^{\star} \hat{\boldsymbol{z}}. \tag{3}$$

Proposition 1. *If a module is a T-module, defined by the tilt angle η, the module is a torque-balanced module.*

Proof. By the definition of a T-module, the tilted rotors are in the axis-angle representation, where $\hat{\boldsymbol{p}}_j = \frac{\boldsymbol{p}_j}{\|\boldsymbol{p}_j\|}$ is the axis of rotation and η_j is the angle that satisfies $\eta_1 = -\eta_2 = \eta_3 = -\eta_4 = \eta$. We apply Rodrigues' rotation formula to obtain the rotation matrix ${}^{M}\boldsymbol{R}_j = \boldsymbol{I}_3 + (\sin \eta_j)\boldsymbol{P}_j + (1 - \cos \eta_j)\boldsymbol{P}_j^2$ from the axis-angle pair $\hat{\boldsymbol{p}}_j, \eta_j$, where $\boldsymbol{P}_j = (\hat{\boldsymbol{p}}_j)^{\times}$. Since a module has a square configuration, we assume $\boldsymbol{p}_1 = [a, a, 0]^{\top}$, $\boldsymbol{p}_2 = [a, -a, 0]^{\top}$, $\boldsymbol{p}_3 = [-a, -a, 0]^{\top}$, and $\boldsymbol{p}_4 = [-a, a, 0]^{\top}$. Replacing ${}^{M}\boldsymbol{R}_j$ in terms of η and a, the left-hand side of (1) simplifies to $2 \sin \eta \, (\boldsymbol{P}_1^2 - \boldsymbol{P}_2^2)\hat{\boldsymbol{z}} = \boldsymbol{0}$. Similarly, we simplify the left-hand side of (2) to $2(1 - \cos \eta)(\boldsymbol{P}_2^2 - \boldsymbol{P}_1^2)\hat{\boldsymbol{z}} = \boldsymbol{0}$. Replacing ${}^{M}\boldsymbol{R}_j$ in (3) shows that $\boldsymbol{R}^{\star} = \boldsymbol{I}_3$. If and only if ${}^{M}\boldsymbol{R}_j = \boldsymbol{I}_3$ for all $j = 1, \ldots, 4$, $\lambda = 4$; otherwise, $\lambda < 4$. □

2 Different Structures and force polytope

The first structure is omnidirectional. The second structure has its force polytope (which is scaled in the x- and y-axes of $\{S\}$ by a factor of 4 for better visualization) thinner than that of the third structure. Although the wider force polytope of the third structure indicates a wider range of tilting in hovering, the maximum payload capacity is less than that of the second, indicated by the smaller "height" of the polytope.

Structure	Force polytope	Description	Characteristics	Applications
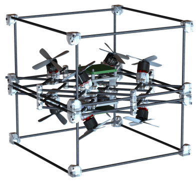	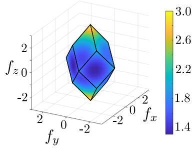	Omnidirectional structure of 2 T-modules with $\eta_1 = \frac{\pi}{4}$ and $\eta_2 = -\frac{\pi}{4}$ connected bottom to bottom.	Ability to hover at an arbitrary attitude with half of the rotors idling.	• 3-D environment imaging. • Maneuvering in cluttered environment.
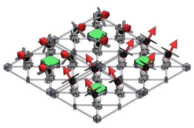	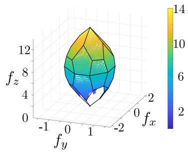	Fully-actuated 2×2 structure composed of 4 R-modules, used for experiment 3.	Ability to generate strong lift force while remaining fully-actuated.	• Transporting heavy packages. • Base station for coverage control.
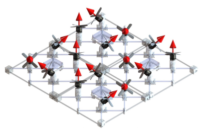	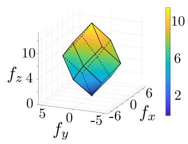	Fully-actuated 2×2 structure of 4 T-modules, used for experiment 4, 5, and 6.	Ability to achieve higher tilt angles when hovering.	• Transporting delicate objects with attitude constraints.
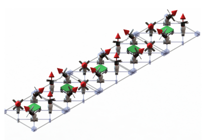	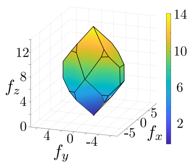	Fully-actuated 5×1 structure of 5 T-modules.	Ability to accelerate in one direction faster than in another.	• Navigating through narrow spaces. • Fixed-direction transportation.
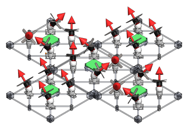	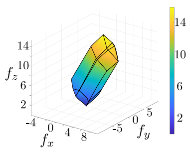	Fully-actuated plus-shape structure composed of 3 T-module of 2 types and 2 R-modules.	Ability to move in cluttered environments such as a half-collapsed building.	• Exploring cluttered environment. • Traversing wind-disturbed fields.

Table 1: Force polytopes of the corresponding H-ModQuad structures. The second and third structures are the fully-actuated structures used for the real-robot experiments.

3 Module components

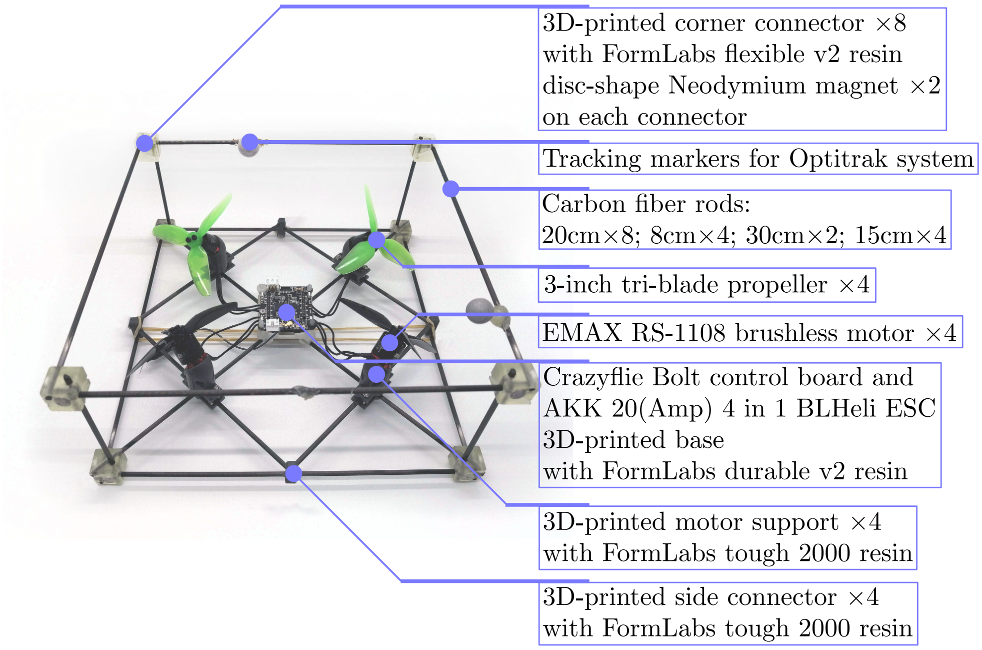

Fig. 1: The main components of an H-ModQuad prototype, exemplified by a T-module.

4 Experiment state plot

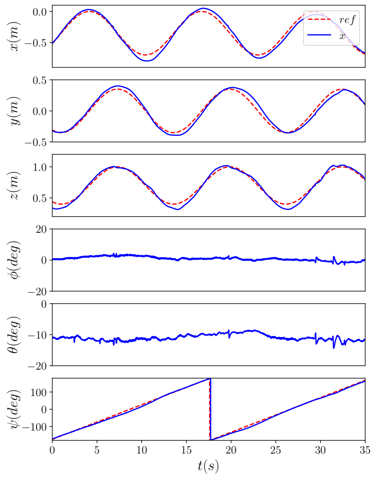

(a) The desired and recorded position and orientation of the structure in Experiment 1.

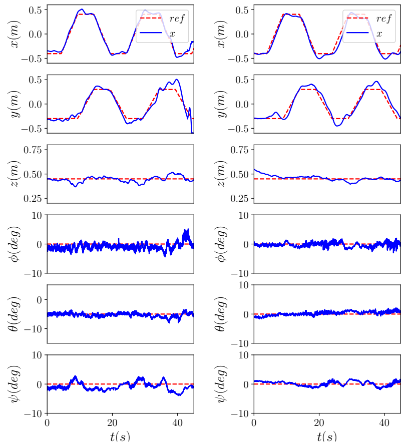

(b) The desired and recorded position and orientation of the structure in Experiment 2, tilted at 5° versus 0°.

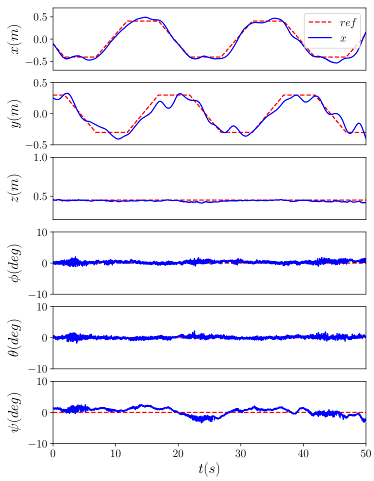

(c) The position and orientation of the structure in Experiment 3, desired versus recorded.

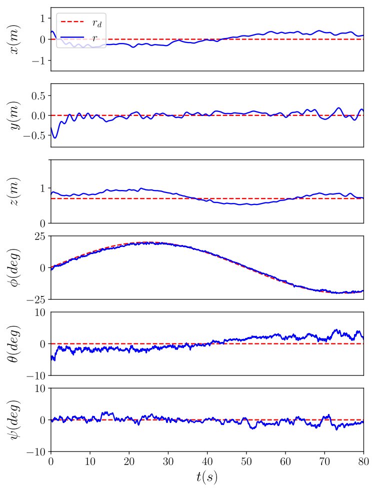

(d) The desired and recorded position and orientation of the structure in Experiment 4.

Fig. 2: The trajectory tracking plots of Experiments 1 - 4.

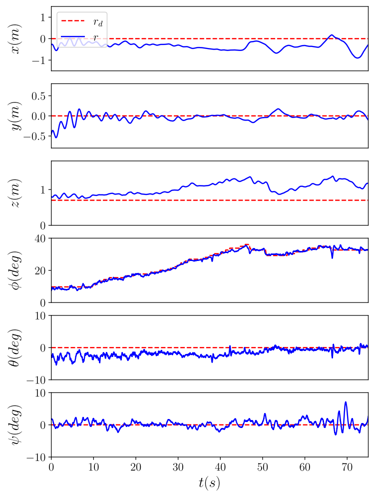

(a) The desired and recorded position and orientation of the structure in Experiment 5.

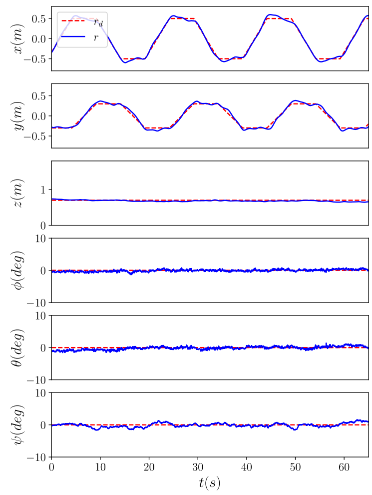

(b) The desired and recorded position and orientation of the structure in Experiment 6.

Fig. 3: The trajectory tracking plots of Experiments 5 and 6.